11th International Symposium on Turbulence and Shear Flow Phenomena (TSFP11)
Southampton, UK, July 30 to August 2, 2019

Numerical study of transition delay in supersonic boundary layers via wavy surfaces

Min Yu

China Academy of Aerospace Aerodynamics
No.17 Yungang West Road, Fengtai District, Beijing
yumin8688@126.com

Zhiyong Liu

China Academy of Aerospace Aerodynamics
No.17 Yungang West Road, Fengtai District, Beijing
liuzhiyongtv@163.com

Wubing Yang

China Academy of Aerospace Aerodynamics
No.17 Yungang West Road, Fengtai District, Beijing
sstmyang@qq.com

ABSTRACT

The influence of a supersonic boundary layer over a flat plate with a wavy surface has been studied by means of numerical simulation and linear stability analysis for the freestream Mach number 4.5. Numerical simulations are conducted for propagation of disturbances introduced at the inlet and effects of the wavy surface. The transition scenarios are compared for smooth wall case and wavy wall cases. The result indicates that the wavy walls showed potential to delay transition. Introduced planar second mode disturbance are damped and some oblique mode disturbances are excited by the wavy surfaces. This paper suggests an effective flow control strategy of using wavy surface to delay transition in supersonic boundary layers.

INTRODUCTION

Laminar-turbulent transition in supersonic boundary layers is a fundamental and important subject in fluid dynamics. Even after lots of studies, transition physics are not entirely understood. This is because numerous possible mechanism and nonlinear interactions exist. At supersonic speed, the unstable modes include first mode, second mode, Görtler mode instability and so on.

The transition issue can be affected by local shaping of the body surface (Hader et al., 2014; Park et al., 2016). Wavy-wall stabilization concept was studied by Bountin et al. (2013) and Egorov et al. (2010) through linear stability theory, two-dimensional DNS and wind tunnel experiments. The results show that the second mode waves of high frequency are stabilized by the concave wavy wall comprising several shallow cavities of a half-sinus shape. They found that the wavy wall could suppress the growth of the second mode in a wide frequency range, so it can be used to delay transition. Zhang et al. (2016) studied the influence of distributed roughness for disturbance evolution in Mach 4.5 flat plate used by stability analysis and numerical simulation. The result indicated that distributed roughness affects the amplitude evolution of disturbance by changing the basis flow field in the boundary layer. Sawaya et al. (2018) performed an assessment of the impact of various two-dimensional surface nonuniformities, and they found that surface nonuniformities are able to reduce the amplitude of disturbances to a certain degree in a boundary layer.

From the view of current research, the study of transition delay is far from sufficient. Previous study is focus on two-dimensional cases. In this paper, the effect of wavy wall on the transition of boundary layer of a Mach 4.5 plate is studied by means of three-dimensional numerical simulation.

NUMERICAL ALGORITHM

The Mach number at the free stream is taken to be 4.5, the gas parameter values are chosen to be those at 5km altitude. The plate surface is set to be isothermal with the temperature T_w =600K. The computational domain starts at X =500mm.

Governing equations

The governing equations are the compressible Navier-Stokes equations in the conservative formulation. The non-dimensional form of the Navier-Stokes equations is

$$\frac{\partial U}{\partial t}+\frac{\partial F_j}{\partial x_j}=\frac{\partial F_{vj}}{\partial x_j} \tag{1}$$

where U denotes the flux, F_j are the convective terms, and F_{vj} are the viscous terms.

The flow filed is calculated by using a high-order-accurate finite-difference code. The governing equations are discretized as below: the 5th-order WENO scheme for the convective terms after Steger-Warming flux splitting, the 6th-order center difference scheme for the viscous terms, and the 3rd-order Runge-Kutta scheme for the time integration.

Boundary conditions are specified as follows. At the inlet, the forcing disturbances are imposed; at the outlet the extrapolated boundary condition is achieved; at the upper boundary, the flow is approximated by the far field at infinity; at the wall, the non-slip condition is imposed.

Disturbances generation

In the controlled transition scenario, the disturbances at the inlet are introduced via the boundary condition:

$$u'=A\hat{u}(y)\,e^{i(\alpha x+\beta z-\omega t)}+c.c. \tag{2}$$

where A is the amplitude, ω is the frequency, $\alpha=\alpha_r+i\alpha_i$ and β is the streamwise and spanwise wavenumber obtained by Orr-Sommerfeld equation, $-\alpha_i$

means the growth rate of the distrubance , $\hat{u}(y)$ is the corresponding eigenvector, and $c.c.$ means the conjugate. Three unstable modes are forced at the inlet, that is, a primary axisymmetric (two-dimensional) second mode disturbance with high amplitude and a pair of oblique (three-dimensional) first mode disturbances with small amplitudes. The specific parameters are shown in table 1. Figure 1 shows the neutral curve at the inlet, and the introduced disturbances are marked with cross symbols. Figure2 shows the linear evolution of the introduced disturbances.

Table 1. Parameters of the disturbances at the inlet

Index	A	ω	α_r	$-\alpha_i$	β
2D	0.010	2.904	3.1835	0.0639	0
3D	0.0001	0.242	0.3320	0.0146	±0.9189

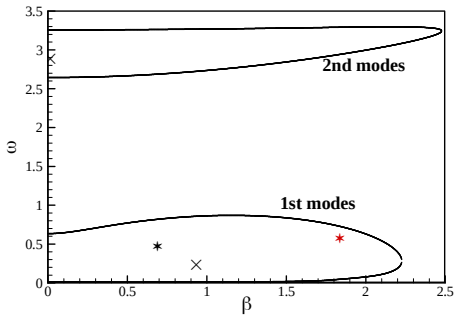

Figure 1. The neutral curve of the modes at the inlet

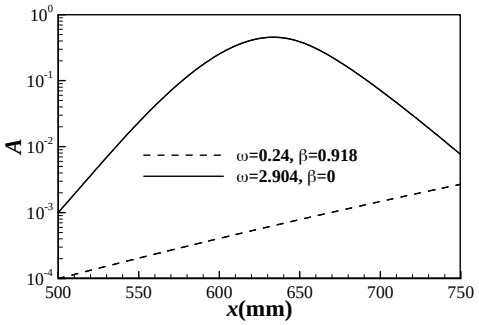

Figure 2. The linear growth development of inlet disturbances

Wavy surface shape

Two surface geometric configurations are used for the study of transition process: (1) flat plates, and (2) wavy plates. Two wavy surface shapes with dimensions are shown in figure3.

- wavy1 surface

Wavy1 surface place at a region from x =530mm to 581.92mm. The shape of the wavy1 surface is assumed in the form:

$$y=\begin{cases}0, & x<x1\\ h\times\sin(kx\times(x-x1))\times\sin(kz\times z), & x1\le x\le x_2\\ 0, & x>x2\end{cases} \quad (3)$$

where h =0.1mm (about 10% local boundary layer thickness), $kx=4\frac{2\pi}{x2-x1}$, $kz=1.5\frac{2\pi}{lz}$, and lz means spanwise length. This shape corresponds to the disturbance with streamwise wavenumber α_r =0.484 and spanwise wavenumber β =0.6891. The disturbance labeled with black star symbol in figure 1.

- wavy2 surface

Wavy2 surface place at a region from x =530mm to 572.23mm. The shape of the wavy2 surface is assumed in the form:

$$y=\begin{cases}0, & x<x1\\ h\times\sin(kx\times(x-x1))\times\sin(kz\times z), & x1\le x\le x_2\\ 0, & x>x2\end{cases} \quad (4)$$

where h =0.1mm, $kx=4\frac{2\pi}{x2-x1}$, $kz=4\frac{2\pi}{lz}$, and lz means spanwise length. This shape corresponds to the disturbance with streamwise wavenumber α_r =0.595 and spanwise wavenumber β =1.8378. This disturbance labeled with red star symbol in figure 1.

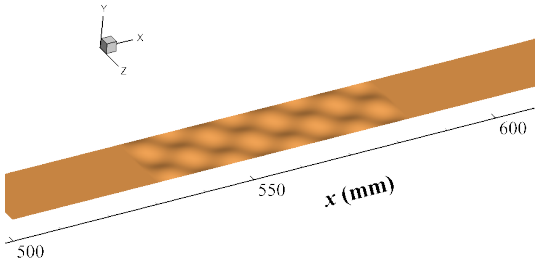

(a) wavy1

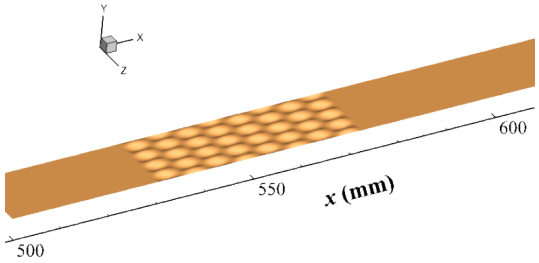

(b) wavy2

Figure 3. The schematic diagram for wavy surfaces

DISCUSSIONS

Preliminaries

Figure 4 shows the phase velocities plot, and the synchronization point where mode F and mode S cross exists for Mach 4.5 flow. The distributions of growth rate of Mode F and S with respect to streamwise location are plotted in figure 5. In the studies of Fong et al. (2014), the location of 2-D roughness element and the synchronization point are important in determining the roughness effect on modal growth. In our study, wavy surface shape located upstream of the synchronization point, so it has the ability to damp perturbations.

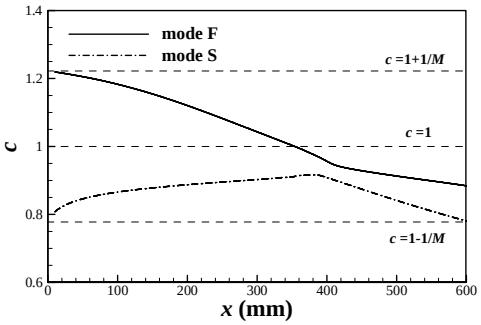

Figure 4. Distributions of phase velocity of mode F and S

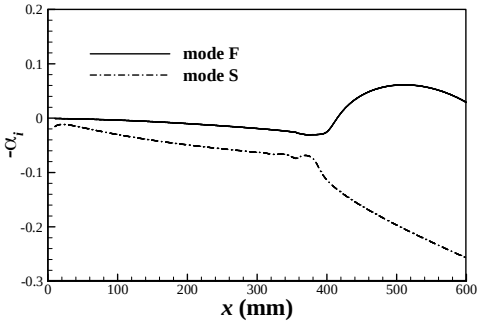

Figure 5. Distributions of growth rate of mode F and S

Skin friction coefficient

The downstream development of time- and spanwise-averaged skin friction coefficient plotted in figure 6. In the presence of the wavy wall, the evolution of skin friction is altered significantly. In the smooth flat wall case, the skin friction follows the laminar curve up to $X \approx 580$mm and then increases to the first peak. The first peak in the skin friction surrounds at $X \approx 600$mm and then causes a dip up to $X \approx 635$mm. Then the skin friction coefficient keeps growing and eventually reaches to saturation at $X \approx 690$mm. This particular development of the skin friction is probably due to the controlled transition simulation where only a few selected waves are forced initially. In the cases of wavy1 and wavy2 walls, the skin friction deviate the laminar curve at $X \approx 700$mm and increase to maximum value at $X \approx 735$mm. It can be concluded that wavy surfaces can effectively delay transition.

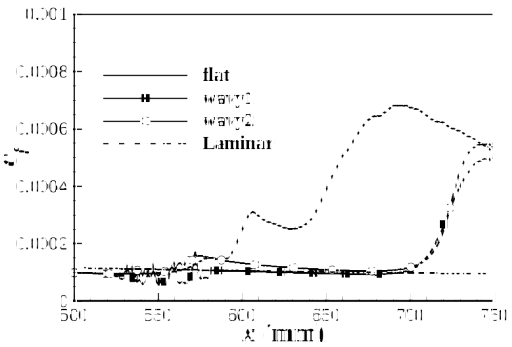

Figure 6. The evolution of skin friction coefficient

Modes evolution

Figure 7 shows the evolution of selected modes by doing Fourier transform in the spanwise direction and time period. The term (h, k) represents the disturbance with the frequency $h\omega_0$ (ω_0=0.242) and spanwise wavenumber $k\beta_0$ (β_0 =0.9189). Mode (12, 0) denotes the introduced primary axisymmetric disturbance, and the evolution of the mode is plotted in figure 7(a). The wavy wall configuration causes a massive reduction of the introduced primary high-frequency disturbance. A close comparison of figure 6 and 7(a) reveals that the location where the primary mode (12, 0) reach its largest amplitude level corresponds to the initial deviation of the skin friction from its laminar value. Mode (1, 1) denotes the introduced oblique disturbance. Mode (13, 1) obtained by the interaction between the introduced mode (12, 0) and (1, 1) is damped. The wavy wall configurations trigger the three-dimensional disturbances (12, 2) which has the same frequency as the introduced two-dimensional disturbance. But the mode (12, 2) only keeps growing a short distance.

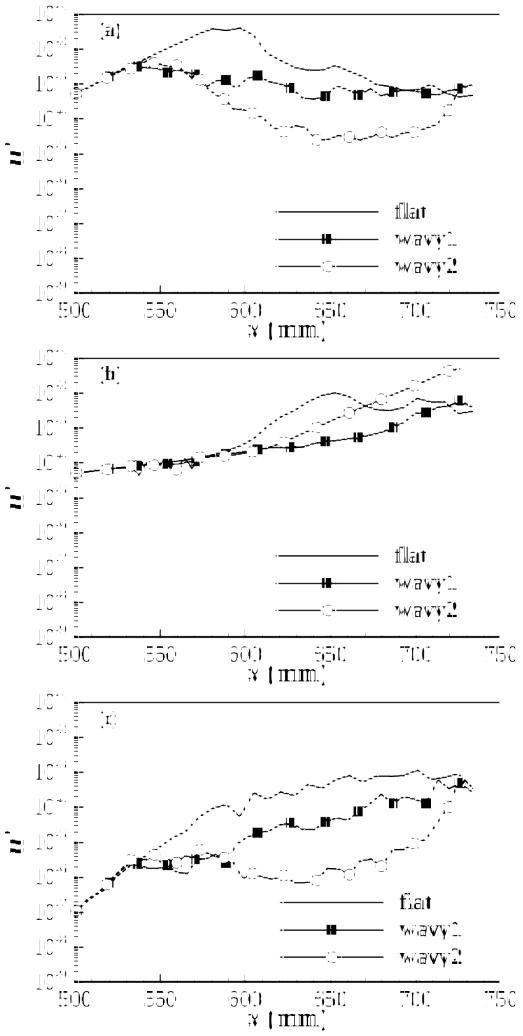

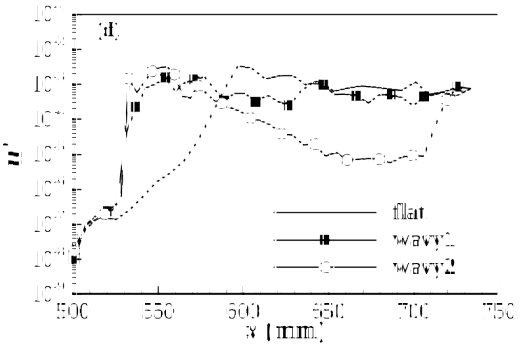

Figure 7. Maximum of streamwise velocity disturbance versus downstream distance (a) (12, 0), (b) (1, 1), (c) (13, 1), (d) (12, 2)

Energy spectra

The energy contained in the temporal and spanwise modes is defined as:

$$E_{uu,t}(k_t, j) = \frac{1}{Nz}\sum_{k_z=1}^{Nz}\hat{u}^2(k_t, j, k_z) \quad (5)$$

$$E_{uu,z}(k_z, j) = \frac{1}{Nt}\sum_{k_t=1}^{Nt}\hat{u}^2(k_t, j, k_z) \quad (6)$$

Where k_t is the frequency, k_z is the spanwise wavenumber, and $\hat{u}$ denotes the wall normal amplitude distribution of the Fourier transformed velocity variables. The energy spectra contained in temporal and spanwise modes are plotted in Figure 8. For the smooth wall case (Figure8 (a) and (b)) the energy spectra become broader as downstream progresses. For x =612.8, the spectra for the temporal modes has a peak value at k_t =2.904 corresponding the introduced 2D disturbance. For x =692.8, the graphs show the energy accumulation is in reasonable agreement with the theoretical predictions indicating that the flow has progressed into the turbulent regime. For wavy wall cases (from figure 8 (c) to (f)), the energy spectrum is lower compared to the smooth wall case. Therefore, one can be concluded that the flow for wavy wall cases has not progressed as far into the turbulent regime as the smooth wall case.

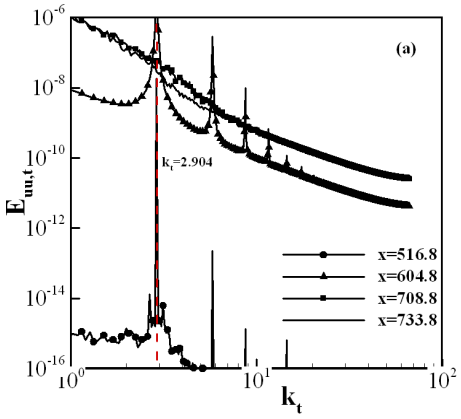

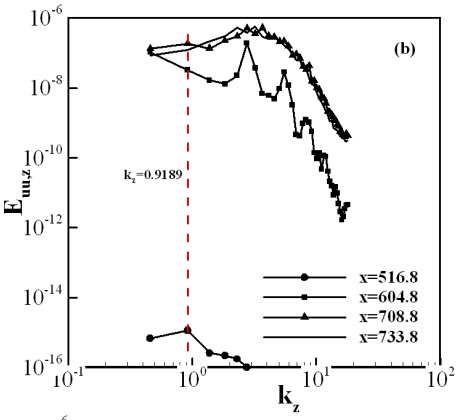

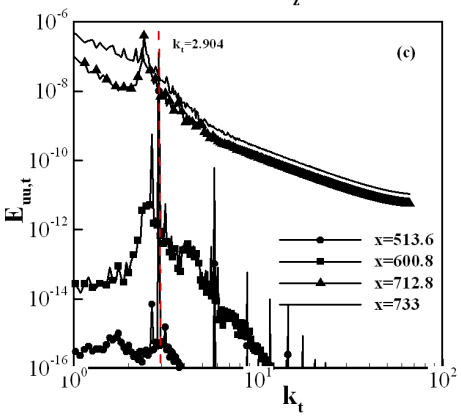

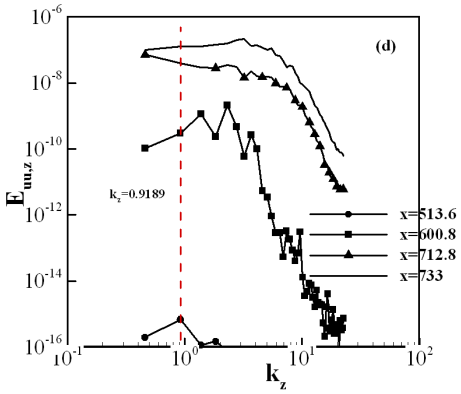

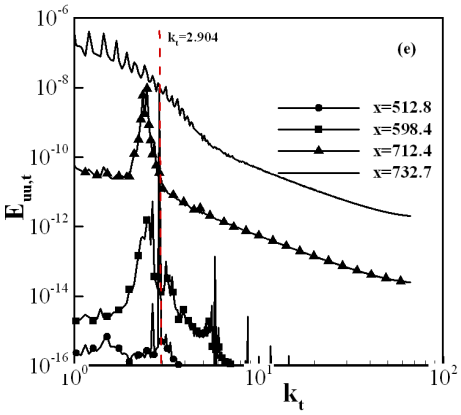

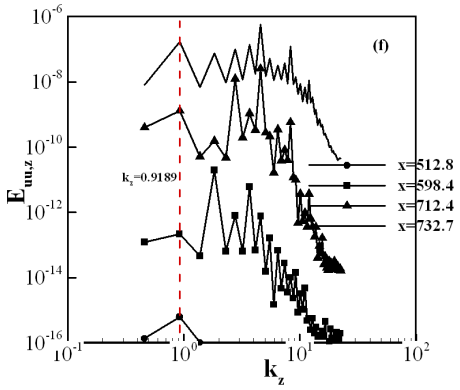

Figure 8. Energy spectra (a) temporal spectrum, smooth wall, (b) spanwise spectrum, smooth wall, (c) temporal spectrum, wavy1 wall, (d) spanwise spectrum, wavy1 wall, (e) temporal spectrum, wavy2 wall, (f) spanwise spectrum, wavy2 wall

LST analysis

Figure 9 shows the profiles of the mean velocity at two different streamwise locations for smooth wall case and wavy wall cases. The neutral curves based on these profiles are obtained by LST (plotted in figure 10). The location X =590mm correspond to the onset of the transition location for smooth wall case. The location from X =550mm to 590mm, the domain of the unstable first modes becomes larger. That means more and more first modes are excited when transition onset. Compared smooth wavy case with wavy wall cases at same location X =590mm, the unstable second modes for wavy wall cases shift to the lower frequency, and the domain of the unstable first modes becomes smaller. It is the resion that he transition location is delayed for wavy wall cases. It indicated that the existence of wavy walls influence the characteristics of meanflow.

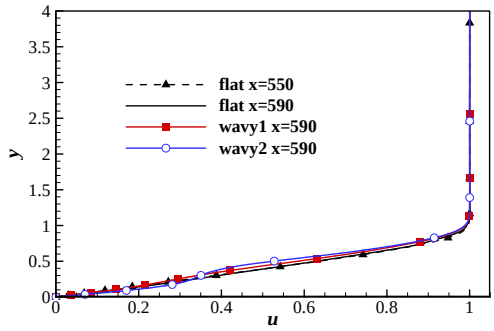

Figure 9. The profiles of mean velocity

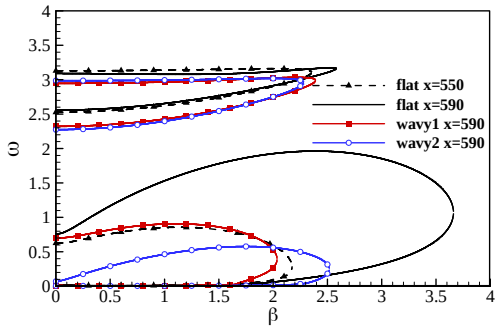

Figure 10. The neutral curves

CONCLUSIONS

The present study is concerned with the influence of a supersonic boundary layer over a plate with a wavy surface. We carried out numerical simulation and stability analysis for the freestream Mach number 4.5 flow. It is effectual to design a wavy surface to impact the onset of transition. Introduced planar second mode disturbance are damped for wavy surfaces cases, and some 3-D disturbances are excited on the region where wavy surface exist. But those disturbances can't keep growing for a long distance. The mean flows are altered by the existence of the wavy walls. Under the wavy walls, the unstable second modes move to lower frequency, while the unstable domain of first modes becomes smaller. So the transition location is eventually delayed for wavy wall cases compared to smooth wall case.

REFERENCES

Hader C., Brehm C., Fasel H. F., 2014, "Numerical investigation of transition delay for various controlled breakdown scenarios in a Mach 6 boundary layer using porous walls", *AIAA Paper*, 2014-2500.

Park, D., Park, S. O., 2016, "Study of Effect of a smooth bump on hypersonic boundary layer instability", *Theoretical and Computational Fluid Dynamics*, Vol. 30, pp. 543-563.

Bountin, D., Chimitov, T., Maslov, A., and et al, 2013, "Stabilization of hypersonic boundary layer using a wavy surface", *AIAA Journal*, Vol. 51(5), pp. 1203-1210.

Egorov, I. V., Novikov, A. V., and Fedorov, A. V., 2010, "Direct numerical simulation of supersonic boundary layer stabilization using grooved wavy surface", *AIAA-Paper*, 2010-1245.

Sawaya, J., Sassanis, V., Yassir S., and Secsu, A., 2018, "Assessment of the impact of two-dimensional wall deformation shape on high-speed boundary-layer disturbances", *AIAA Journal*.

Zhang, C. B., Luo, J. S., Gao, J., 2016, "Effects of distributed roughness on Mach 4.5 boundary-layer transition", *Journal of Aerospace Power* (in Chinese), Vol. 5, pp. 1234-1241.

Fong, K. D., Wang, X. W., Huang, Y., and et al, 2015, "Second mode suppression in hypersonic boundarylayer by roughness: design and experiments", *AIAA Journal*, Vol. 53, pp. 3138-3144.